

# Wave-packet spreading dynamics under a noninstantaneous nonlinearity: Self-trapping, defocusing, and focusing

Marcelo L. Lyra and Rodrigo P. A. Lima

*Instituto de Física, Universidade Federal de Alagoas 57072-970 Maceió, Alagoas, Brazil*

(Received 3 February 2012; published 14 May 2012)

Special localized wave modes show up in several physical scenarios including BEC in optical lattices, nonlinear photonic crystals, and systems with strong electron-phonon interaction. These result from an underlying nonlinear contribution to the wave equation that is usually assumed to be instantaneous. Here we demonstrate that the relaxation process of the nonlinearity has a profound impact in the wave-packet dynamics and in the formation of localized modes. We illustrate this phenomenology by considering the one-electron wave packet spreading in a C60 buckball structure whose dynamics is governed by a discrete nonlinear Schrödinger equation with a Debye relaxation of the nonlinearity. We report the full phase diagram related to the spacial extension of the asymptotic wave packet and unveil a complex wave-packet dynamical behavior.

DOI: [10.1103/PhysRevE.85.057201](https://doi.org/10.1103/PhysRevE.85.057201)

PACS number(s): 05.45.-a, 71.30.+h, 73.20.Mf, 73.61.Wp

## I. INTRODUCTION

The discrete nonlinear Schrödinger equation (DNSE) has been frequently used to describe a wealth of nonlinear physical phenomena associated with wave dynamics. The DNSE can display a large class of topologically stable solutions such as solitons, vortex rings, and breathers [1–6]. These solutions have been largely explored in the context of Bose-Einstein condensates in optical lattices and light propagation in photonic crystals [7–10]. The DNSE also captures some features related to the electron-phonon interaction that can be effectively taken into account by a nonlinear term in the electronic Hamiltonian [11]. Nonlinearity was shown to breakdown the Anderson localization in low-dimensional disordered systems by promoting a diffusive-like spread of the electronic wave packet [12].

The self-trapping of the wave function is one of the most remarkable effects associated with the presence of a nonlinear contribution to the discrete Schrödinger equation. An initially localized wave packet spreads in the regime of weak nonlinearities, but becomes trapped around its initial position when the nonlinear coupling is above a threshold value [13–15]. The self-trapping transition has been characterized in one-dimensional and two-dimensional systems. The critical nonlinear coupling is of the order of the energy bandwidth for an initial wave packet fully localized in a single site of a linear chain. In two-dimensional lattices, it increases as the initial wave packet becomes wider [16]. Recently, the influence of the nonlinear response time on the self-trapping transition has been investigated in one-dimensional systems. By considering a delayed nonlinearity, it has been shown that the critical nonlinearity depends nonmonotonically on the response time [17]. When the relaxation of the nonlinearity is described by a Debye process, the typical response time drastically affects the wave-packet dynamics. Much weaker nonlinearities are needed to trap the wave packet [18]. It focalizes after an initial spread exhibiting pronounced finite-size effects including wave-packet fragmentation. The relaxation of the nonlinearity also leads to the wave-packet relocalization in disordered systems [19,20].

The wave-packet dynamics in nonlinear honeycomb and some closely related lattices has been a subject of intense recent investigations. These have been mainly motivated by

the ability to buildup optical lattices and photonic crystals with these topologies, which allows the experimental observation of several theoretically predicted phenomena, such as topology-induced bistability [21], discrete localized modes and breathers [22,23], conical diffraction [24,25], self-trapping of vortices, gap vortices, and gap solitons [26]. Nonlinearity is also expected to play a significant role in the dynamics of electronic wave packets in carbon-based structures [27,28]. Recent experiments have probed the electron-phonon interaction in graphene which can account for an effective nonlinearity [29]. Low-temperature scanning tunneling spectroscopy experiments have been recently used to map the wave function in graphene quantum dots [30], which opens the possibility to experimentally observe many theoretically predicted nonlinear effects in low-dimensional carbon-based structures. However, most of the previous theoretical studies of nonlinear wave dynamics in two-dimensional lattices do not include finite-size effects and the relaxation of the nonlinearity which might play important roles in nanoscaled structures.

In the present work, we show that both finite-size and finite response-time effects have a strong impact on the wave-packet spreading dynamics. We will follow the time evolution of an initially fully localized wave packet whose propagation is governed by a DNSE with Debye relaxation of the nonlinearity. To illustrate the phenomenology, we consider the wave-packet evolution over a C60 buckball. In this topology, all sites are equivalent and the absence of borders avoids the superposition of surface effects to the finite-size ones. We will report the phase diagram in the two-dimensional parameter space (nonlinear coupling  $\chi$  and response time  $\tau$ ), which unfolds a quite complex structure with three distinct localized phases.

## II. MODEL AND METHODS

A nonlinear contribution for the one-electron Schrödinger equation results from the underlying electron-phonon interaction [11–16]. Within the adiabatic approximation, such a nonlinear term can be considered as instantaneous. Going beyond the adiabatic approximation, the effective nonlinear term has been shown to obey a Debye relaxation process [31]. Within a tight-binding approach and considering a localized

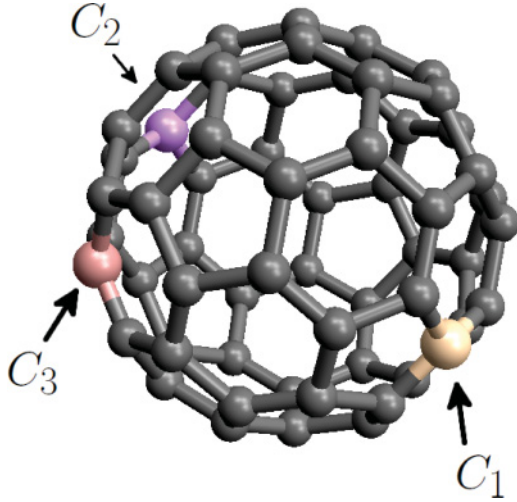


FIG. 1. (Color online) Schematic representation of the C60 buckball. Each site has two hexagon-hexagon bonds and one hexagon-pentagon bond.  $C_1$  represents the site at which the wave packet is fully localized at  $t = 0$ .  $C_2$  is the site diametrically opposite to the initial position.  $C_3$  stands for the site targeted in Fig. 3(d).

orbitals basis, the dynamics of a one-electron wave packet can be described by a DNSE with a relaxing nonlinearity, written as

$$i\dot{\Psi}_n(t) = \varepsilon_n \Psi_n(t) + \sum_m V_{nm} \Psi_m(t) - X_n(t) \Psi_n(t), \quad (1)$$

$$\dot{X}_n(t) = -\frac{1}{\tau} [X_n(t) + \chi |\Psi_n(t)|^2], \quad (2)$$

where we used  $\hbar = 1$ .  $\Psi_n(t)$  is the coefficient of the wave vector expanded in the localized orbitals basis  $|\Psi(t)\rangle = \sum_n \Psi_n(t) |n\rangle$ . The relaxing nonlinearity  $X(t)$  is considered to have a typical response time  $\tau$  and strength coefficient  $\chi$ . The sum is taken over first-neighbor pairs of sites  $(n, m)$  that are coupled by a hopping amplitude  $V_{nm}$ .  $\varepsilon_n$ 's represent the on-site energies. In the limit of  $\tau \rightarrow 0$ , the nonlinearity becomes instantaneous  $X_n(t) = -\chi |\Psi_n(t)|^2$  and the usual DNSE is recovered.

In what follows, we will solve the above nonlinear dynamical equations for an initially localized wave packet  $\Psi_n(t=0) = \delta_{n,1}$ . We will consider a C60 buckball topology (see Fig. 1), which is composed of 20 hexagons and 12 pentagons. Each of the 60 equivalent sites has three bonds. Two of them are between a hexagon and a pentagon and the remaining one between two hexagons. In the real C60 molecule, the hexagon-hexagon bonds are slightly shorter than the hexagon-pentagon bonds. This feature ultimately leads to a small difference in the corresponding hopping amplitudes which we will not consider in the present work. We will take  $V_{nm} = V$  for every bond and will work in units of  $V = 1$ . Further, we can also consider  $\varepsilon_n = 0$  without any loss of generality. The dynamical equations were solved using a standard eighth-order Runge-Kutta algorithm and the norm conservation was followed with a precision of  $10^{-8}$  to ensure the numerical accuracy.

To characterize the spacial extension of the wave packet, we computed the participation function defined as

$$P(t) = \left[ \sum_{n=1}^N |\Psi_n(t)|^4 \right]^{-1}, \quad (3)$$

which gives a measure of the fraction of the lattice sites at which the wave packet is spread at time  $t$ . It becomes equal to  $N$  for a uniformly distributed wave packet. For a fully localized state  $P = 1$ .

We also computed the wave packet average energy  $E = \langle \Psi | H | \Psi \rangle$ , which can be written in the localized orbitals basis as

$$E = \langle \Psi | H | \Psi \rangle = \sum_n i \Psi_n^*(t) \dot{\Psi}_n(t). \quad (4)$$

The energy time evolution over a finite disordered nonlinear one-dimensional lattice has been recently used to characterize the subdiffusive wave-packet spreading [32,33] and to explain the wave-packet relocalization due to the relaxation of the nonlinearity [20].

### III. RESULTS

We followed the time evolution of the wave packet until it reached a statistically stationary regime. We explored the two-dimensional parameter space  $(\tau, \chi)$  to buildup the phase diagram regarding the spacial extension of the asymptotic wave packet in the regime of a focusing nonlinearity  $\chi > 0$ . Four distinct phases were identified, as reported in Fig. 2. There is a single extended phase, on which the wave packet spreads uniformly over all sites of the buckball, and three distinct localized phases. The extended phase prevails in the regime of weak nonlinearities. However, narrow branches of the extended phase are found between localized phases. While

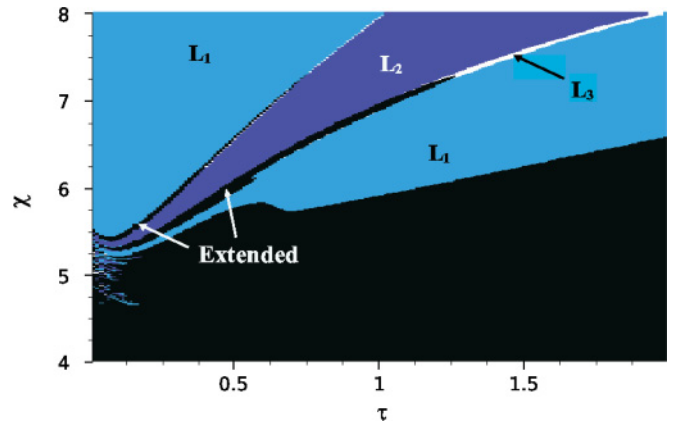


FIG. 2. (Color online) Phase diagram concerning the spacial extension of the asymptotic wave packet in the  $(\tau, \chi)$  parameter space. The extended phase with a uniformly distributed wave packet occurs at small nonlinearities and two branches (black region).  $L_1$  [light blue (light gray)] corresponds to a phase with the wave packet localized around its initial position.  $L_2$  [dark blue (dark gray)] is the phase where the localization is concentrated in the site diametrically opposite to the initial position. In the narrow  $L_3$  (white) phase, the wave packet localizes in other sites. A complex sequence of localization-delocalization transitions is observed at small  $\tau$  values and intermediate nonlinear strengths.

these extended branches die out when the relaxation time increases, the main extended phase becomes wider.

The predominant localized phase  $L_1$  corresponds to an asymptotic wave packet that results localized mostly at the initial position (site labeled  $C_1$  in Fig. 1). In this region, we found the participation number to become slightly above unit with the probability density concentrated at the initial position. There are two main regions of the parameter space on which the wave packet becomes trapped on the initial position. A second localized phase  $L_2$  appears in between these two  $L_1$  regions. In this new localized phase, the participation function is of the same order as in the localized phase  $L_1$ . However, the probability density is centered at the site that is diametrically opposite to the initial position (labeled as  $C_2$  in Fig. 1). The two branches of the extended phase are in between these two localized phases. A third localized phase  $L_3$  occurs in between  $L_1$  and  $L_2$ . In this narrow phase, the wave packet was found to become localized around other positions besides the initial and the diametrically opposite sites. A complex sequence of localization-delocalization transitions takes place at small values of the relaxation time when one crosses the regime of intermediate nonlinear strengths.

To follow the wave-packet dynamics on these distinct phases, we plot the time evolution of the participation

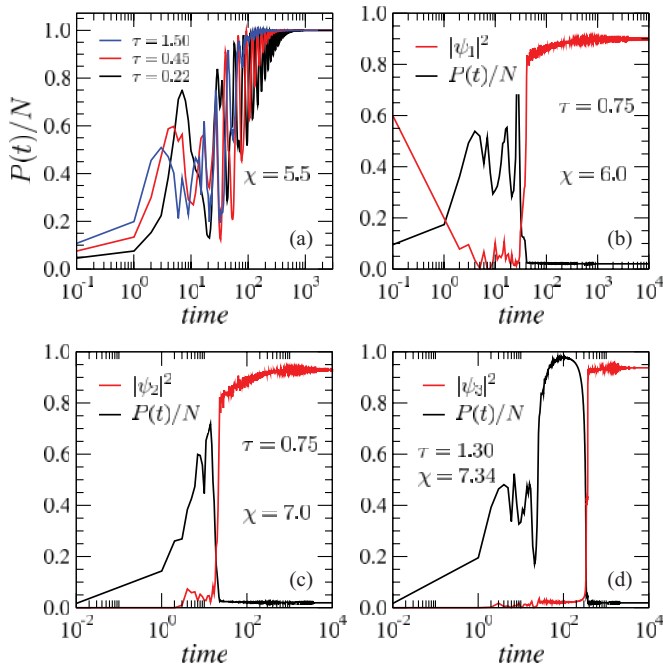


FIG. 3. (Color online) Time evolution of the normalized participation number  $P/N$  [black lines in (b), (c), and (d)] and the relevant occupancy probabilities  $|\Psi_i(t)|^2$  [red (gray) lines in (b), (c), and (d)] for representative values of the physical parameters. (a) Extended phase:  $\chi = 5.5$  and  $\tau = 0.22, 0.45$ , and  $1.50$  (from right to left) being, respectively, on the first, second, and third extended regions. Notice that the expanding wave packet develops breathing oscillations. (b) Localized  $L_1$  phase: after the initial expansion, the wave packet self-focuses and relocalizes around its initial position. (c) Localized  $L_2$  phase: the wave packet relocalization occurs around the site diametrically opposite to its initial position. Localized  $L_3$  phase: the relocalization occurs around the site labeled as  $C_3$  in Fig. 1.

function and the relevant occupation probabilities for some representative values of the parameters, as shown in Fig. 3. The dynamics in the extended phase is illustrated in Fig. 3(a) for parameter values covering the two branches and the main extended region. The normalized participation function converges to  $P/N = 1$  indicating that the asymptotic wave packet is uniformly distributed over all buckball sites. The convergence to this state is achieved after an oscillatory (breathing) transient regime.

In Fig. 3(b) we depict the typical wave-packet dynamics in the  $L_1$  localized phase. We show the time evolution of both the participation number and the occupancy probability of the initial site  $|\Psi_1(t)|^2$ . In the initial transient, the wave packet spreads in an oscillatory fashion and occupies a finite fraction of the buckball sites. After this transient, the wave packet self-focuses and relocalizes. The increase of  $|\Psi_1(t)|^2$  indicates that the wave packet relocalizes around its initial position. A very similar phenomenon occurs in the localized phases  $L_2$  and  $L_3$ , as illustrated in Figs. 3(c) and 3(d), respectively. However, the self-focusing drives the wave packet toward the site diametrically opposite to its initial position in phase  $L_2$ . In the localized  $L_3$  phase, the wave packet spreads almost uniformly over the lattice before starting to self-focus. In this case, the position of the asymptotic localized state is very sensitive to values of the physical parameters. For the values used in Fig. 3(d), the wave packet relocalizes around the site labeled as  $C_3$  in Fig. 1.

We report the time evolution of the wave-packet energy in Fig. 4. For the initial condition used in our study (a fully localized state and vanishing nonlinearity), the wave-packet initial energy is  $E = 0$ . The relaxation process of the nonlinearity promotes an energy drift [20]. In Fig. 4(a), we show the energy time evolution for three cases corresponding to asymptotically extended wave packets. In all cases, the wave-packet energy evolves toward a value slightly above  $E = 3$ . This is consistent with Fig. 3(a) that shows the asymptotic wave packet uniformly spreading over the lattice. The nearest-neighbors hopping terms are responsible for the main wave-packet energy (these account for  $E = 3$ ). The nonlinear term gives a small correction to the energy in the case

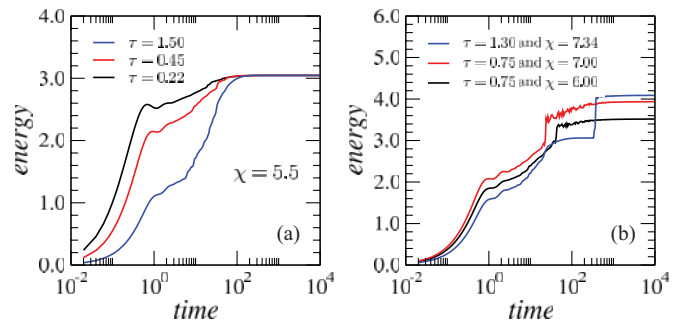


FIG. 4. (Color online) (a) Time evolution of the energy for three representative cases of an asymptotically extended wave packet (decreasing values of  $\tau$  from left to right). The convergence to a value close to  $E = 3$  is consistent with a uniformly extended state. (b) The same for the three cases of localized states shown in Figs. 3(b)–3(d) [decreasing values of  $\chi$  from top to bottom in the long-time regime]. The energy becomes larger than in the localized phase reflecting the predominant role played by the nonlinear contribution.

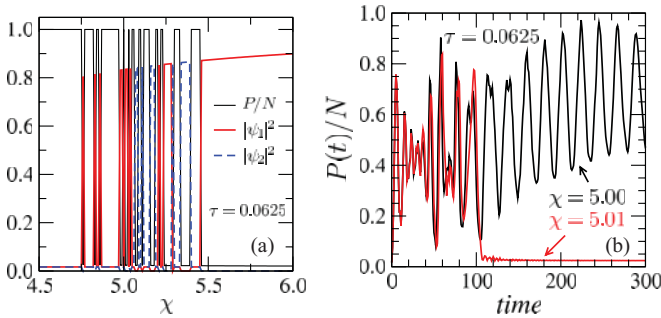


FIG. 5. (Color online) (a) Asymptotic normalized participation function  $P/N$  (black curve) and occupancy probabilities  $|\Psi_i(t)|^2$  at the initial ( $i = 1$ ) [red (gray) solid curve] and diametrically opposite ( $i = 2$ ) [dashed curve] sites as a function of the nonlinear coupling for  $\tau = 0.0625$ . The system depicts a complex sequence of localization and delocalization transitions. (b) The time evolution of the normalized participation function for  $\tau = 0.0625$  and two slightly different nonlinear strengths. Notice a dynamical transition that leads to distinct phases.

of an extended wave packet. In Fig. 4(b), we show the energy time evolution for the same three cases of asymptotically localized states addressed in Figs. 3(b) through 3(d). One can observe that the wave-packet energy develops a plateau during the time period on which it remains spread over the lattice. After this intermediate regime, a dynamic transition leads to the ultimate localization reflected by the fast increase of the wave-packet energy as the nonlinear contribution becomes predominant.

Finally, we closely analyze the wave-packet dynamics in the parameter region where a complex sequence of localization-delocalization transitions occurs within the main extended region (see Fig. 5). We first plot the asymptotic normalized participation function and occupancy probabilities of the initial and diametrically opposite sites as a function of the nonlinear coupling and a fixed relaxation time  $\tau = 0.0625$ , as shown in Fig. 5(a).  $P/N = 1$  in the extended phase, as expected for a uniformly delocalized wave packet. However, before the ultimate localization transition that traps the wave packet around its initial position, a complex sequence of localization-delocalization transitions takes place. The position of the localized wave packet appears to randomly jump between the initial and diametrically opposite sites. For other small values of the relaxation time, we verified that the wave packet can eventually relocalize around other sites. The high sensitivity of the wave-packet dynamics on the precise values of the parameters in this region is illustrated in Fig. 5(b). One observes that, while the orbits of two cases with slightly different parameters remain quite close to each other during some time, a dynamical transition takes them apart. It is worth recalling that a similar dynamical transition has been

previously reported to occur in a two-level system driven by a relaxation process of the nonlinearity [31].

#### IV. SUMMARY AND CONCLUSION

In summary, we showed that the wave-packet spreading dynamics displays a rich phenomenology including self-trapping, defocusing, and focusing when the relaxation process of an effective third-order nonlinearity is taken into account. A C60 buckball structure was used to illustrate this phenomenology. By considering a fully localized initial state, we provided the phase diagram for the spacial extension of the long-time wave packet. The phase diagram shows a complex structure with three distinct phases of localized wave packets, besides the extended phase in which the wave packet spreads uniformly over all buckball sites. In the localized phases, the wave packet was shown to relocalize after an initial spreading over a finite fraction of the network sites. Besides the usual relocalization of the wave packet around its initial position, focalization on the diametrically opposite site takes place in a large stripe of the phase diagram. A narrow phase where the wave packet relocalizes around other sites was also identified. A complex sequence of localization-delocalization transitions was shown to occur at small relaxation times as a function of the nonlinear coupling. These were associated to a dynamical transition which is strongly sensitive to the parameter values in this region. A stability analysis of the stationary states would be to shed light on the underlying mechanism that drives these transitions.

The main aspects of the here-reported phenomenology are expected to show up in general nonlinear physical systems where the wave-packet dynamics are driven by a relaxation process of an underlying nonlinearity. These include electronic states in nanosized clusters with strong electron-phonon coupling, BEC in optical lattices, and light propagation in nonlinear photonic crystals. The present work leaves open the quest of investigating the possible influence of open boundaries and saturation effects that might also be relevant in optical and BEC experiments in finite planar lattices. Further efforts would be to evaluate the relative relevance of these ingredients to the wave-packet dynamics in the presence of a relaxing nonlinearity.

#### ACKNOWLEDGMENTS

We would like to thank CAPES via project PPCP-Mercosul, CNPq, and FINEP (Brazilian Research Agencies) as well as FAPEAL (Alagoas State Research Agency) for partial financial support. We also would like to thank the kind hospitality of the Facultad de Matemática, Astronomía y Física (FaMaF) of Universidad Nacional de Córdoba where part of this work was developed.

- [1] O. Braun and Yu. S. Kivshar, *Phys. Rep.* **306**, 1 (1998).  
 [2] D. Hennig and G. P. Tsironis, *Phys. Rep.* **307**, 333 (1999).  
 [3] A. R. Bishop, G. Kalosakas, K. Ø. Rasmussen, and P. G. Kevrekidis, *Chaos* **13**, 588 (2003).  
 [4] E. Arévalo, *Phys. Rev. Lett.* **102**, 224102 (2009).

- [5] K. J. H. Law, D. Song, P. G. Kevrekidis, J. Xu, and Zhigang Chen, *Phys. Rev. A* **80**, 063817 (2009).  
 [6] C. Gaul, E. Díaz, R. P. A. Lima, F. Domínguez-Adame, and C. A. Müller, *Phys. Rev. A* **84**, 053627 (2011).

- [7] E. Díaz, C. Gaul, R. P. A. Lima, F. Domínguez-Adame, and C. A. Müller, *Phys. Rev. A* **81**, 051607(R) (2010).
- [8] B. B. Wang, P. M. Fu, J. Liu, and B. Wu, *Phys. Rev. A* **74**, 063610 (2006).
- [9] J.-K. Xue and A.-X. Zhang, *Phys. Rev. Lett.* **101**, 180401 (2008).
- [10] S. A. Ponomarenko and G. P. Agrawal, *Phys. Rev. Lett.* **97**, 013901 (2006).
- [11] C. A. Bustamante and M. I. Molina, *Phys. Rev. B* **62**, 15287 (2000); G. P. Tsironis, M. I. Molina, and D. Hennig, *Phys. Rev. E* **50**, 2365 (1994).
- [12] A. S. Pikovsky and D. L. Shepelyansky, *Phys. Rev. Lett.* **100**, 094101 (2008); G. Kopidakis, S. Komineas, S. Flach, and S. Aubry, *ibid.* **100**, 084103 (2008); S. Flach, D. O. Krimer, and Ch. Skokos, *ibid.* **102**, 024101 (2009); Ch. Skokos, D. O. Krimer, S. Komineas, and S. Flach, *Phys. Rev. E* **79**, 056211 (2009).
- [13] M. Johansson, M. Hornquist, and R. Riklund, *Phys. Rev. B* **52**, 231 (1995).
- [14] P. K. Datta and K. Kundu, *Phys. Rev. B* **53**, 14929 (1996).
- [15] Z. Pan, S. Xiong, and C. Gong, *Phys. Rev. E* **56**, 4744 (1997).
- [16] W. S. Dias, M. L. Lyra, and F. A. B. F. de Moura, *Phys. Rev. B* **82**, 233102 (2010).
- [17] F. A. B. F. de Moura, I. Gléria, I. F. dos Santos, and M. L. Lyra, *Phys. Rev. Lett.* **103**, 096401 (2009).
- [18] F. A. B. F. de Moura, E. J. G. G. Vidal, I. Gléria, and M. L. Lyra, *Phys. Lett. A* **374**, 4152 (2010).
- [19] R. A. Caetano, F. A. B. F. de Moura, and M. L. Lyra, *Eur. Phys. J. B* **80**, 321 (2011).
- [20] M. Mulansky and A. Pikovsky, *Eur. J. Phys. B* **85**, 1 (2012).
- [21] M. I. Molina and Y. S. Kivshar, *Opt. Lett.* **35**, 2895 (2010).
- [22] K. J. H. Law, P. G. Kevrekidis, V. Koukouloyannis, I. Kourakis, D. J. Frantzeskakis, and A. R. Bishop, *Phys. Rev. E* **78**, 066610 (2008).
- [23] H. Leblond, B. A. Malomed, and D. Mihalache, *Phys. Rev. A* **83**, 063825 (2011).
- [24] M. J. Ablowitz, S. D. Nixon, and Y. Zhu, *Phys. Rev. A* **79**, 053830 (2009).
- [25] O. Bahat-Treidel, O. Peleg, M. Segev, and H. Buljan, *Phys. Rev. A* **82**, 013830 (2010).
- [26] K. J. H. Law, A. Saxena, P. G. Kevrekidis, and A. R. Bishop, *Phys. Rev. A* **79**, 053818 (2009).
- [27] B. Hartmann and W. J. Zakrzewski, *Phys. Rev. B* **68**, 184302 (2003).
- [28] Y. Brihaye and B. Hartmann, *J. Phys. A: Math. Gen.* **37**, 1181 (2004).
- [29] M. Bianchi, E. D. L. Rienks, S. Lizzit, A. Baraldi, R. Balog, L. Hornekaer, and Ph. Hofmann, *Phys. Rev. B* **81**, 041403 (2010); A. Grüneis, C. Attacalite, A. Rubio, D. V. Vyalikh, S. L. Molodtsov, J. Fink, R. Follath, W. Eberhardt, B. Büchner, and T. Pichler, *ibid.* **79**, 205106 (2009).
- [30] D. Subramaniam, F. Libisch, Y. Li, C. Pauly, V. Geringer, R. Reiter, T. Mashoff, M. Liebmann, J. Burgdörfer, C. Busse, T. Michely, R. Mazzarello, M. Pratzner, and M. Morgenstern, *Phys. Rev. Lett.* **108**, 046801 (2012); S. H. Park, J. Borme, A. L. Vanegas, M. Corbetta, D. Sander, and J. Kirschner, *ACS Nano* **5**, 8162 (2011); S. K. Hämäläinen, Z. Sun, M. P. Boneschanscher, A. Uppstu, M. Ijäs, A. Harju, D. Vanmaekelbergh, and P. Liljeroth, *Phys. Rev. Lett.* **107**, 236803 (2011).
- [31] V. M. Kenkre and H.-L. Wu, *Phys. Rev. B* **39**, 6907 (1989); P. Grigolini, H.-L. Wu, and V. M. Kenkre, *ibid.* **40**, 7045 (1989).
- [32] M. Mulansky, K. Ahnert, A. Pikovsky, and D. L. Shepelyansky, *Phys. Rev. E* **80**, 056212 (2009).
- [33] T. Terao, *Phys. Rev. E* **83**, 056611 (2011).